

# Numerical study of a thermoacoustic refrigerator with different stack geometries

Prastowo Murti<sup>1</sup>, Wijayanti Dwi Astuti<sup>2\*</sup>, Burhan Febrinawarta<sup>1</sup>, Arief Putra Pratama<sup>1</sup>

<sup>1</sup> Department of Mechanical and Industrial Engineering, Universitas Gadjah Mada, Indonesia

<sup>2</sup> Department of Electrical Engineering and Informatics, Universitas Gadjah Mada, Indonesia

E-mail: wijayanti.dwi.a@ugm.ac.id \*

\* Corresponding Author

## ABSTRACT

This study examines the performance of a thermoacoustic refrigerator with various stack geometries as a potential eco-friendly alternative to conventional refrigeration systems that rely on chlorofluorocarbons (CFCs). Thermoacoustic refrigerators create a cooling effect using sound waves and environmentally friendly gases such as helium. The stack, a crucial component where energy conversion occurs, must be optimized to maximize cooling efficiency. However, no studies have previously investigated the impact of stack geometries under a uniform system configuration. Thus, this study aims to numerically evaluate how different stack geometries and materials affect the performance of thermoacoustic refrigerators while maintaining consistent system geometry and properties to ensure fair comparison. The research focuses on three types of stack geometries: parallel plate, ceramic honeycomb, and wire mesh screen. Using DeltaEC software, the performance of these stacks was analyzed with a constant hydraulic radius. The results show that the wire mesh screen stack provides the highest cooling power (330 W) and coefficient of performance (COP) of 0.81, outperforming the other geometries. These findings highlight the potential of optimized stack designs to improve the efficiency of thermoacoustic refrigerators, promoting their development as a sustainable cooling technology.

This is an open-access article under the [CC-BY-SA](#) license.



## ARTICLE INFO

### Article history

Received:

24 May 2025

Revised:

18 July 2025

Accepted:

18 August 2025

### Keywords

geometries  
numerical  
refrigerator  
stack  
thermoacoustic

## 1. Introduction

The use of chlorofluorocarbons (CFCs), commonly known as Freon, has been prevalent in refrigeration and air conditioning. Initially regarded as safe and effective cooling agents, CFCs have since been identified as significant contributors to ozone layer depletion and global warming. Scientific research has established that CFCs are persistent in the atmosphere, leading to their accumulation and subsequent breakdown by ultraviolet radiation, which releases chlorine atoms that catalyze the destruction of ozone molecules in the stratosphere [1]. Due to the concerns associated with its environmental impact, this research seeks to explore the development of thermoacoustic devices as a potential solution to mitigate the harmful effects of Freon gas. Specifically, the study focuses on thermoacoustic refrigeration systems that utilize environmentally friendly working gases such as air and noble gases as refrigerants. These systems offer several advantages, including high reliability, cost-effectiveness, environmental friendliness, and the absence of moving parts (e.g., compressors) [2].

Figure 1 illustrates a thermoacoustic refrigeration comprising a drive, a resonator tube, heat exchangers, and a stack. The heat exchangers facilitate the transfer of heat into and out of the thermoacoustic device. When the driver is turned on [3,4], the reciprocating motion of the driver membrane induces oscillations between compression and rarefaction phases within the stack. During

compression, the gas particles move closer together, increasing pressure and temperature locally. Conversely, during rarefaction, the gas particles move apart, decreasing pressure and temperature. This oscillatory movement leads to the transfer of heat from one side of the stack to the other, creating a temperature gradient along the length of the stack [2,5]. The continuous oscillation of the gas, driven by the sound waves, maintains the temperature gradient, allowing the cooler side of the stack to act as a refrigeration source [2].

The stack is a critical component in thermoacoustic refrigeration, as it is the site of energy conversion, which must be optimized to achieve maximum cooling efficiency. Previous studies by researchers have explored the use of various stack geometries to enhance the performance of thermoacoustic refrigerators such as parallel plate [6], ceramic honeycomb catalyst [7], wire mesh screen stainless steel [8], and pile of wool stainless steel [9]. However, these investigations were conducted with differing thermoacoustic system dimensions, complicating the identification of an optimal stack geometries. To tackle this issue, the current study seeks to assess how various stack geometries and materials influence the performance of thermoacoustic refrigerators, while keeping the system geometry and specific properties, particularly the hydraulic radius ( $r_h$ ), consistent to ensure a fair comparison. The hydraulic radius, which is the ratio of the flow's cross-sectional area to the wetted perimeter, plays a crucial role in the interaction between the oscillating gas and the stack material. This radius significantly impacts the viscous and thermal boundary layers within the stack, which are essential for efficient thermoacoustic processes [2]. The performance analysis of thermoacoustic refrigerator will be conducted using DeltaEC software, a tool widely utilized by the thermoacoustic community for the design and optimization of thermoacoustic devices [2,8,10,11]. The result showed that stack made of wire mesh screen achieved highest COP among all stacks.

## 2. Method

A standing wave thermoacoustic refrigerator is schematically depicted in Fig. 1, consisting of a driver, resonator, stack, and heat exchangers. A Hofler thermoacoustic refrigerator configuration was employed due to its well-known high cooling performance [12], where a closed resonator tube and a stack are positioned near the loudspeaker. At the opposite end, a resonator sphere (compliance) was attached, enabling the loudspeaker to generate a standing wave with a quarter-wavelength within the resonator tube. The total length of the resonator, including the driver and its housing, was 1007 mm. In this study, the driver utilized was the B&C 8BG51, produced by B&C Speakers, with the specifications detailed is presented in Table 1 [13,14].

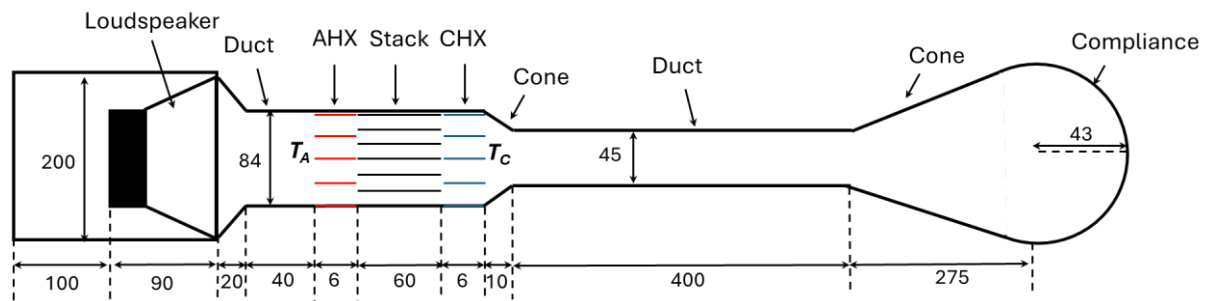


**Fig. 1.** Schematic diagram of standing-wave thermoacoustic model (dimension in mm).

Short parallel plate-shaped heat exchangers were employed to help heat transfer into and out of the system. One heat exchanger, known as the cold heat exchanger (CHX) with the temperature of  $T_C$ , absorbs heat from the environment, providing cooling to the surrounding area, while the other, called the ambient heat exchanger (AHX) with the temperature of  $T_A$ , dissipates heat to the environment.

**Table 1.** Specifications of loudspeakers B&C 8BG51 [13,14].

Parameter	Value
$R_m$ (kg/s)	0.95
$m$ (kg)	0.035
$K_m$ (N/m)	3814
$R_e$ ( $\Omega$ )	5.1
$Bl$ (Tm)	11.8
$L_e$ (H)	0.0005
$f_0$ (Hz)	52
$X_{max}$ (mm)	6.5
$\eta_{max}$ (%)	69.2
$A_d$ (m <sup>2</sup> )	0.022

In this study, three different geometries of stacks were employed, as shown in Fig. 2. To ensure a fair comparison, we set the hydraulic radius ( $r_h$ ) of stacks to be similar. This value of  $r_h$  can be achieved by these three geometries of stacks using equation shown in Table 2. The first stack was parallel plate stack (Fig. 2(a)) made of mylar with a thickness ( $l$ ) of 0.045 mm and a plate spacing ( $2y_0$ ) of 1.49 mm, resulting in a hydraulic radius of 0.745 mm. The second stack was a cylindrical ceramic honeycomb catalyst support (Fig. 2(b)), which had square pores with a side ( $P$ ) of 1.49 mm, resulting in a hydraulic radius of 0.745 mm. The last stack was made of wire mesh screen (Fig. 2(c)) with wire diameter ( $D$ ) of 0.38 mm and mesh number ( $m$ ) of 10, resulting in a hydraulic radius of 0.713 mm.

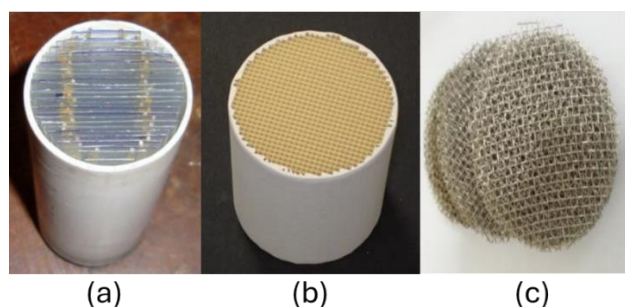


**Fig. 2.** (a) Parallel plate stack [15], (b) Ceramic honeycomb catalyst [16], and (c) wire mesh screen [17].

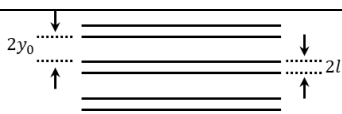
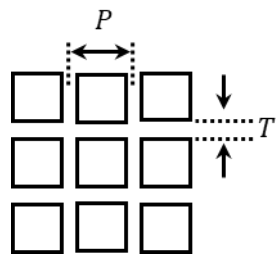
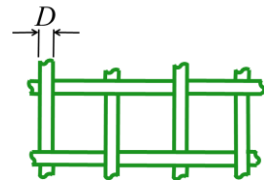
A thermoacoustic refrigerator is simulated using DeltaEC software, which numerically solves the one-dimensional acoustic wave equations for a selected gas within a specified geometry. The model allows for the application of acoustic, thermal, or geometrical boundary conditions through the use of guess and target pairs. DeltaEC employs a shooting algorithm to adjust the guessed variables to meet user-defined targets that can be distributed throughout the device. With the basic thermoacoustic

refrigerator segments (loudspeaker, stack, duct, heat exchangers, and compliance) in the previous section, a DeltaEC model was created. The shooting algorithm was then utilized to determine the remaining unknown system parameters, such as the optimal length of the cold duct, within the given constraints. The boundary conditions of this model were as follows: the working fluid was helium at 5 atm, the resonance frequency was forced to be 350 Hz, the temperature of the AHX ( $T_A$ ) was 290 K, and the acoustic pressure at the end of the compliance was at a maximum while the acoustic velocity was at a minimum (zero). The coefficient of performance COP of a refrigerator is defined as

$$COP = \frac{Q_C}{W_L} \quad (1)$$

where  $Q_C$  is the cooling power and  $W_L$  is the acoustic power used to pump  $Q_C$ . The cooling power  $Q_C$  is the ability to remove heat from the space around it. Higher cooling power means the refrigerator can handle a larger load or cool the space more rapidly.

**Table 2.** Geometry of stack and its hydraulic radius equation.

Stack Geometry		Hydraulic Radius Equation	Value (mm)	Porosity (-)
Parallel Plate		$r_h = y_0$	0.745	0.94
Ceramic Honeycomb Catalyst		$r_h = \frac{P - T}{2}$	0.745	0.68
Wire Mesh Screen		$r_h = \frac{D \left(1 - \frac{\pi m D}{4}\right)}{\pi m D}$ $m = \text{number of openings/inches}$	0.713	0.88

### 3. Results and Discussion

Simulations were conducted with varying levels of electric power input to the loudspeaker to increase the acoustic power utilized by the stack for heat transfer, leading to a temperature difference across the stack. Fig. 3 illustrates the effect of electric power input  $W_L$  on the temperature difference across the stack ( $T_A - T_C$ ) under no-load condition and different stack geometries and materials. This is done because  $W_L$  induces high-amplitude gas oscillations, which are necessary to generate the temperature difference ( $T_A - T_C$ ). It can be observed that an increase in electric power leads to an increase in the temperature difference ( $T_A - T_C$ ) for all stacks. This behaviour is expected, as  $T_A - T_C$  is proportional to amplitude of gas oscillations increased by increasing  $W_L$  [2,18]. Additionally, at low  $W_L$ , the

rectangular stack generates the highest  $T_A - T_C$  among the stacks. However, at high  $W_L$ , the screen stack produces the highest  $T_A - T_C$ , reaching around 32°C. At low  $W_L$ , the oscillation of the working gas is influenced by the stack's porosity, with the rectangular stack having a lower porosity than the others. High porosity leads to greater viscous losses, which, in turn, affect heat transfer within the stack. At high  $W_L$ , however, porosity does not impact  $T_A - T_C$ , indicating a nonlinear behaviour that falls outside the scope of this study.

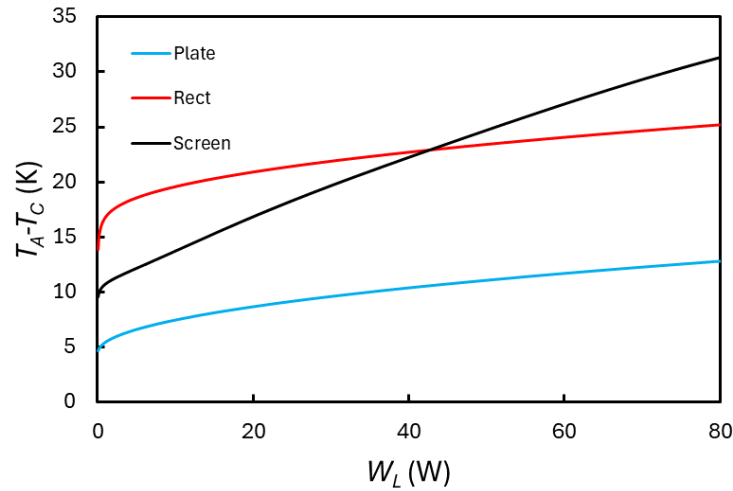


**Fig. 3.** Temperature of the cold heat exchanger as function of the electric power supplied to the loudspeaker.

The superior performance of the screen stack is confirmed by Fig. 4, which illustrates the acoustic power absorption by the stack as a function of  $W_L$ . It is evident that from the initial stages of  $W_L$ , the screen stack absorbed more acoustic power to transferring heat across the stack than all other stacks. Additionally, we found that the material type of the stack significantly affects heat transfer. Stacks with lower thermal conductivity have more difficulty transferring heat, which results in greater heat transfer through the air rather than through the stack. Conversely, stacks with high specific heat capacity absorb more heat from the air

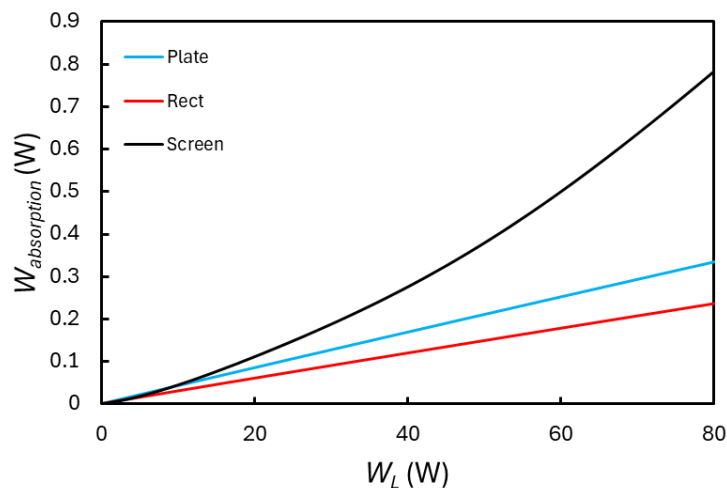


**Fig. 4.** Acoustic power ( $W_{absorption}$ ) along the stack as function of the electric power supplied to the loudspeaker.

. Consequently, the screen stack mad of stainless steel absorbs more heat but experiences less heat loss compared to other stacks. This ultimately leads to a higher  $T_A - T_C$  for the screen stack compared to other stacks. To measure the performance of the thermoacoustic refrigerator, we need to apply a load to the cold heat exchanger. Fig. 5 shows the cold heat exchanger temperature ( $T_C$ ) as a function of the cooling power ( $Q_C$ ). In this study, we set the maximum  $T_C$  at 288 K or 15°C, as this temperature is recommended for storing shelf-stable foods[19]. As shown in Fig. 5, the plate stack was only able to generate a  $Q_C$  of 50 W, whereas the rectangular stack was able to generate a  $Q_C$  of 240 W. The highest  $Q_C$ , around 330 W, was achieved when the thermoacoustic refrigerator used the screen stack. This result is in line with Fig. 3, which indicates that the screen stack is preferable as a stack in a thermoacoustic refrigerator.

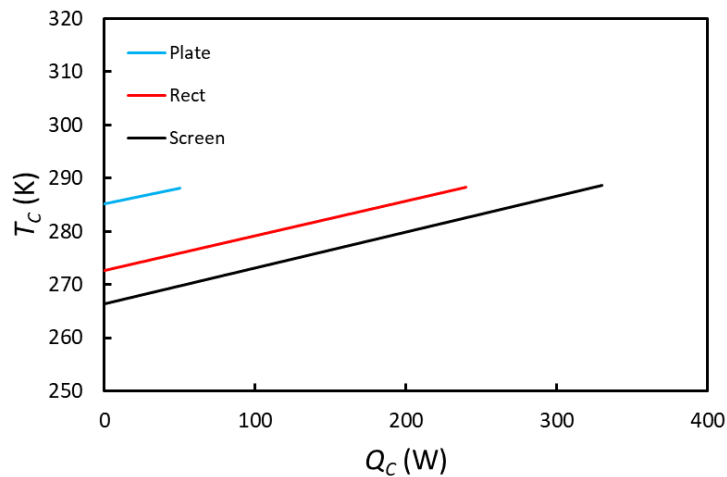


**Fig. 5.** Temperature of cold heat exchanger (CHX)  $T_C$  as function of the cooling power  $Q_C$ .

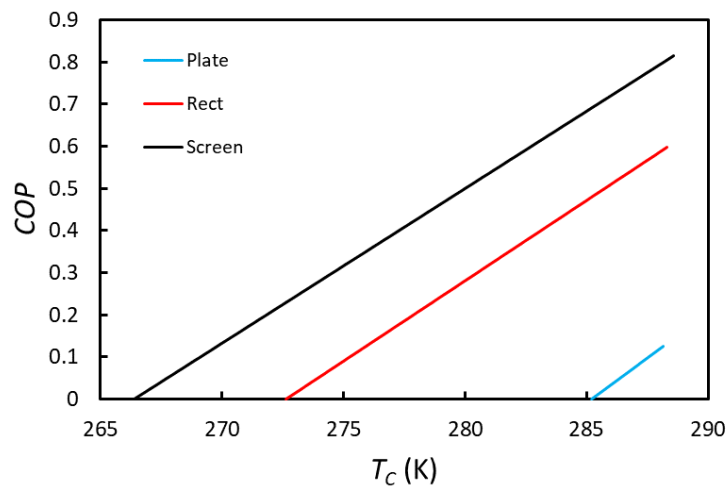


**Fig. 6.** COP as function of cold heat exchanger  $T_C$ .

Fig. 6 shows the performance measurements COP as a function of cold heat exchanger temperature  $T_C$ . As can be seen from Fig. 6, the COP increases as the heat load increases for stacks. Stack screen as it generated lowest temperature, it produced the highest COP to reach 0.81. Therefore, the findings underscore the importance of stack design in optimizing thermoacoustic refrigeration systems, particularly for enhancing efficiency and achieving better cooling performance.

#### 4. Conclusion

This study highlights the significant impact of stack geometry on the performance of thermoacoustic refrigerators. Previous research faced challenges in identifying the optimal stack geometry due to variations in system configurations. To address this, the current study utilized DeltaEC software to evaluate different stack geometries under consistent conditions. The findings reveal that the wire mesh screen stack outperformed other geometries, achieving the highest temperature difference and coefficient of performance. Its superior acoustic and thermal properties make the wire mesh screen stack the most effective choice for enhancing the cooling performance of thermoacoustic refrigeration systems. These results underscore the potential of thermoacoustic devices as a sustainable and environmentally friendly alternative to conventional cooling technologies, supporting further research and development in this field.

#### Acknowledgment

This research was funded by the Academic Excellence Improvement Scheme C Program Universitas Gadjah Mada Number 6530/UN1.P1/PT.01.03/2024.

#### References

- [1] Molina, M. J., & Rowland, F. S. (1974). Stratospheric sink for chlorofluoromethanes: Chlorine atom-catalysed destruction of ozone. *Nature*, 249(5460). <https://doi.org/10.1038/249810a0>
- [2] Swift, G. W. (2017). Thermoacoustics: A Unifying perspective for some engines and refrigerators: Second edition. In *Thermoacoustics: A Unifying Perspective for Some Engines and Refrigerators: Second Edition*. <https://doi.org/10.1007/978-3-319-66933-5>
- [3] Setiawan, I., & Sifa, M. (2020). The construction and testing of an acoustic energy harvester consisting of a Helmholtz resonator and a loudspeaker. *Journal of Physics: Theories and Applications*, 4(1). <https://doi.org/10.20961/jphys theor-appl.v4i1.47587>
- [4] Setiawan, I., Wibowo, B. W., & Prasetya, R. D. (2023). Experimental Study of Storing Electrical Energy Generated by an Acoustic Energy Harvester Into a Supercapacitor. *INDONESIAN JOURNAL OF APPLIED PHYSICS*, 13(2). <https://doi.org/10.13057/ijap.v13i2.67671>
- [5] Tijani, M. E. H., Zeegers, J. C. H., & de Waele, A. T. A. M. (2002). The optimal stack spacing for thermoacoustic refrigeration. *The Journal of the Acoustical Society of America*, 112(1). <https://doi.org/10.1121/1.1487842>
- [6] Backhaus, S., & Swift, G. W. (2001). Fabrication and use of parallel plate regenerators in thermoacoustic engines. *Proceedings of the Intersociety Energy Conversion Engineering Conference, I*.
- [7] Ueda, Y., Mehdi, B. M., Tsuji, K., & Akisawa, A. (2010). Optimization of the regenerator of a traveling-wave thermoacoustic refrigerator. *Journal of Applied Physics*, 107(3). <https://doi.org/10.1063/1.3294616>
- [8] Backhaus, S., & Swift, G. W. (2000). A thermoacoustic-Stirling heat engine: Detailed study. *The Journal of the Acoustical Society of America*, 107(6). <https://doi.org/10.1121/1.429343>
- [9] Abduljalil, A. S., Yu, Z., & Jaworski, A. J. (2009). Experimental characterisation of low-cost regenerators for travelling-wave thermoacoustic devices. *7th International Energy Conversion Engineering Conference*. <https://doi.org/10.2514/6.2009-4580>



- [10] Murti, P., Takizawa, A., Shoji, E., & Biwa, T. (2022). Design guideline for multi-cylinder-type liquid-piston Stirling engine. *Applied Thermal Engineering*, 200. <https://doi.org/10.1016/j.applthermaleng.2021.117635>
- [11] Murti, P., Shoji, E., & Biwa, T. (2023). Analysis of multi-cylinder type liquid piston Stirling cooler. *Applied Thermal Engineering*, 219. <https://doi.org/10.1016/j.applthermaleng.2022.119403>
- [12] Hofler, T. J., Adeff, J. A., & Atchley, A. A. (1997). Experimental results with a thermoacoustically driven thermoacoustic refrigerator. *The Journal of the Acoustical Society of America*, 101(5\_Supplement). <https://doi.org/10.1121/1.418547>
- [13] Chen, B., Yousif, A. A., Riley, P. H., & Hann, D. B. (2012). Development and Assessment of Thermoacoustic Generators Operating by Waste Heat from Cooking Stove. *Engineering*, 04(12). <https://doi.org/10.4236/eng.2012.412113>
- [14] Piccolo, A. (2018). Design issues and performance analysis of a two-stage standing wave thermoacoustic electricity generator. *Sustainable Energy Technologies and Assessments*, 26. <https://doi.org/10.1016/j.seta.2016.10.011>
- [15] Ikhsan, S., Agung, Bambang S. U., Makoto, N., & Masafumi, K. (2012, November 18). Effects of the Length and Location of Stack on the Temperature Decrease of a Thermoacoustic Cooler. *Conference: 3rd International Conference on Physics 2012*.
- [16] Teruyuki, K., Kyuichi, Y., Masaki, Y., Kazumi, K., & Shin-ichi, S. (2014). Study of a stack made by a 3D printer in the thermoacoustic system. *Proceedings of Symposium on Ultrasonic Electronics*, Vol. 35 (2014), 123–124.
- [17] Murti, P., Setiawan, I., Fadly, M., & Murtyas, S. D. (2018). Pengaruh Jejari Hidrolik Regenerator Dan Frekuensi Gelombang Bunyi Terhadap Kinerja Pompa Kalor Termoakustik Gelombang .... *Jurnal Teknologi*, 10(2).
- [18] Atchley, A. A. (1992). Standing wave analysis of a thermoacoustic prime mover below onset of self-oscillation. *The Journal of the Acoustical Society of America*, 92(5). <https://doi.org/10.1121/1.404355>
- [19] Wibowo, S., Buvé, C., Hendrickx, M., Van Loey, A., & Grauwet, T. (2018). Integrated science-based approach to study quality changes of shelf-stable food products during storage: A proof of concept on orange and mango juices. In *Trends in Food Science and Technology* (Vol. 73). <https://doi.org/10.1016/j.tifs.2018.01.006>